Journal for ImmunoTherapy of Cancer

Cross-cohort analysis identified an immune checkpoint-based signature to predict the clinical outcomes of neuroblastoma

Liang Zeng,[1] Hui Xu ,[1] Shu-Hua Li,[2] Shuo-Yu Xu,[3,4] Kai Chen,[1] Liang-Jun Qin,[1] Lei Miao,[5] Fang Wang,[6] Ling Deng,[6] Feng-Hua Wang,[7] Le Li,[7] Sha Fu,[8] Na Liu,[9] Ran Wang,[10] Ying-Qing Li,[11] Hai-Yun Wang [1,5]

To cite: Zeng L, Xu H, Li S-H, *et al*. Cross-cohort analysis identified an immune checkpoint-based signature to predict the clinical outcomes of neuroblastoma. *Journal for ImmunoTherapy of Cancer* 2023;**11**:e005980. doi:10.1136/jitc-2022-005980

► Additional supplemental material is published online only. To view, please visit the journal online (http://dx.doi.org/10.1136/jitc-2022-005980).

LZ, HX, S-HL and S-YX contributed equally.

Accepted 16 April 2023

For numbered affiliations see end of article.

Correspondence to
Professor Hai-Yun Wang; wanghy29@mail3.sysu.edu.cn

Dr Ying-Qing Li; liyingq1@sysucc.org.cn

Dr Ran Wang; wangr55@mail.sysu.edu.cn

ABSTRACT

Background Neuroblastoma (NB) places a substantial health burden on families worldwide. This study aimed to develop an immune checkpoint-based signature (ICS) based on the expression of immune checkpoints to better assess patient survival risk and potentially guide patient selection for immunotherapy of NB.

Methods Immunohistochemistry integrated with digital pathology was used to determine the expression levels of 9 immune checkpoints in 212 tumor tissues used as the discovery set. The GSE85047 dataset (n=272) was used as a validation set in this study. In the discovery set, the ICS was constructed using a random forest algorithm and confirmed in the validation set to predict overall survival (OS) and event-free survival (EFS). Kaplan-Meier curves with a log-rank test were drawn to compare the survival differences. A receiver operating characteristic (ROC) curve was applied to calculate the area under the curve (AUC).

Results Seven immune checkpoints, including PD-L1, B7-H3, IDO1, VISTA, T-cell immunoglobulin and mucin domain containing-3 (TIM-3), inducible costimulatory molecule (ICOS) and costimulatory molecule 40 (OX40), were identified as abnormally expressed in NB in the discovery set. OX40, B7-H3, ICOS and TIM-3 were eventually selected for the ICS model in the discovery set, and 89 patients with high risk had an inferior OS (HR 15.91, 95% CI 8.87 to 28.55, p<0.001) and EFS (HR 4.30, 95% CI 2.80 to 6.62, p<0.001). Furthermore, the prognostic value of the ICS was confirmed in the validation set (p<0.001). Multivariate Cox regression analysis demonstrated that age and the ICS were independent risk factors for OS in the discovery set (HR 6.17, 95% CI 1.78 to 21.29 and HR 1.18, 95% CI 1.12 to 1.25, respectively). Furthermore, nomogram A combining the ICS and age demonstrated significantly better prognostic value than age alone in predicting the patients' 1-year, 3-year and 5-year OS in the discovery set (1 year: AUC, 0.891 (95% CI 0.797 to 0.985) vs 0.675 (95% CI 0.592 to 0.758); 3 years: 0.875 (95% CI 0.817 to 0.933) vs 0.701 (95% CI 0.645 to 0.758); 5 years: 0.898 (95% CI 0.851 to 0.940) vs 0.724 (95% CI 0.673 to 0.775), respectively), which was confirmed in the validation set.

Conclusions We propose an ICS that significantly differentiates between low-risk and high-risk patients, which might add prognostic value to age and provide clues for immunotherapy in NB.

WHAT IS ALREADY KNOWN ON THIS TOPIC

⇒ Immune checkpoint inhibitor treatment is still considered a promising strategy in neuroblastoma (NB) patients despite the patients' low tumor mutational burden.

WHAT THIS STUDY ADDS

⇒ We propose an immune checkpoint-based signature model based on the expression of immune checkpoints to predict patients' outcomes as well as provide clues for the novel implementation of immunotherapy in NB patients.

HOW THIS STUDY MIGHT AFFECT RESEARCH, PRACTICE OR POLICY

⇒ This study represents the first comprehensive expression landscape of immune checkpoints in NB and their potential use as indicators for immunotherapy in NB.

INTRODUCTION

Neuroblastoma (NB), an extremely heterogeneous disease, is the most common extracranial solid tumor in childhood. Currently, NB patients are stratified into low-risk, intermediate-risk and high-risk groups according to the revised 2021 Children's Oncology Group (COG) risk classifier based on their clinical stage, tumor cell ploidy and MYCN oncogene amplification.[1 2] However, advances in multimodal anticancer therapies that combine surgery, chemotherapy, radiation and antidisialoganglioside (GD2) mAb-based immunotherapy have not significantly improved the survival rates of children with high-risk NB. Thus, there is an urgent need to identify novel and effective therapeutics to improve patient outcomes.[3]

Recent studies have shown that tumors may use a tumor microenvironment (TME) program as a mechanism of immune evasion and to resist chemotherapy and immune checkpoint inhibitors (ICIs).[4] Most immune checkpoints, such as LAG-3, costimulatory molecule 40 (OX40) and programmed death ligand 1 (PD-L1), abnormally expressed on tumors or tumor-infiltrating lymphocytes (TILs) and their clinical significance have been demonstrated in some adult cancers.[5–7] High expression levels of indoleamine-pyrrole 2,3-dioxygenase 1 (IDO1) in cancer have been shown to inhibit natural killer cell function, prevent the activation of effector T cells and promote the emergence of regulatory T cells. Another study showed that T-cell immunoglobulin and mucin domain containing-3 (TIM-3) blockade increases the exposure of intratumoral CD8+T cells to cDC1-derived cytokines, which has implications for the design of therapeutic strategies using antibodies against TIM-3, which are associated with longer progression-free survival and/or overall survival (OS) in urothelial carcinoma.[8] These results indicate that the TME is intricate and that immune checkpoints, such as B7-H3, lymphocyte activation gene 3 (LAG3) VISTA and inducible costimulatory molecule (ICOS), might coexist. Although the low tumor mutational burden in NB patients is a major obstacle for implementing ICIs and only a small proportion of TILs shows tumor reactivity,[9] blocking immune checkpoints is still considered a promising strategy for treating NB patients and is directly associated with improved clinical outcomes.[10] However, the expression levels of these immune checkpoints in NB are still unclear, and there is a need to systematically evaluate their expression status and the relationship between their expression level and clinical outcomes.

Therefore, we performed immunohistochemistry (IHC) to identify the expression levels of the most important immune checkpoints through digital pathology in NB patients and evaluated the prognostic value of each immune checkpoint. Then, we constructed an immune checkpoint-based signature (ICS) for predicting clinical outcomes. Furthermore, we validated the prognostic value of the ICS in an external dataset, which might provide a basis for immunotherapy targets in NB.

METHODS

Clinical samples

In this study, we obtained archived tumor tissues from 212 NB patients treated between January 2012 and December 2020 at two academic institutions, the Guangzhou Women and Children's Medical Center (Guangzhou, China, n=120) and the First Affiliated Hospital of Sun Yat-sen University (Guangzhou, China, n=92). All diagnoses were pathologically confirmed and restaged according to the International Neuroblastoma Staging System (INSS).[11] The COG risk classification of each patient was applied based on their medical records. In addition, the NB gene expression dataset GSE85047 is available from the Gene Expression Omnibus database (http://www.ncbi.nlm.nih.gov/geo). The exclusion criteria were incomplete data of clinical features, mainly including age at diagnosis, INSS, the MYCN status and follow-up data; after applying these criteria, the dataset contained 272 NB samples. Table 1 displays the NB patients' clinical and tumor characteristics in the discovery and validation sets. This study was performed following the Reporting Recommendations for Tumor Marker Prognostic Studies guidelines.[12]

Antibodies used and IHC

The following nine immune checkpoints were chosen for IHC staining: B7-H4, LAG3, PD-L1, B7-H3, IDO1, VISTA, TIM-3, ICOS and OX40. Briefly, pathological sequential slides of 4 µm thickness were sectioned from formalin-fixed, paraffin-embedded (FFPE) tumor blocks and used for IHC analysis as previously described.[13] The primary antibodies used are listed in the online supplemental materials. Representative images of the IHC staining of all these markers are shown in online supplemental figure S1.

Digital image analysis

Physical glass slides of IHC-stained tissue samples with good staining quality were digitized with a scan resolution of 0.24 µm/pixel (Pannoramic Scan 150, 3DHistech, Hungary). Two experienced pathologists (LZ and KC) manually delineated the tumor bulk and excluded necrotic areas (QuPath V.0.2.3, University of Edinburgh, Scotland).[14] All pathological images were autoexamined using a digital analysis. The details are listed in the online supplemental materials.

Random forest for ICS construction

We applied a machine learning random survival forest algorithm to select the most powerful prognostic features of all seven immune checkpoints and then constructed an ICS for predicting the survival of NB patients. This algorithm considers the potential combined effects of the expression level of immune checkpoints in a non-linear, non-parametric manner to identify individuals who are dead or alive. Eventually, the top four immune checkpoints, OX40, B7-H3, ICOS and TIM-3, were selected for the model (online supplemental figure S2). The detailed information is summarized in the online supplemental materials.

Cut-off value

We used the 'Survminer' package in R software (V.4.1.2) and undertook the minimum p value approach to determine whether there were thresholds for the seven immune checkpoint expression levels and risk score of the ICS that independently altered the NB patients' risk of OS.[15] Online supplemental figure S3 shows that the smallest statistically significant p value was an optimal threshold that independently predicted the patients' risk of death. Based on the optimal threshold, each patient was given a binary score, that is, 0 for low expression/risk and 1 for high expression/risk for each immune checkpoint and the ICS, respectively.

Table 1 Clinicopathologic characteristics of NB patients in the discovery and validation sets stratified by the ICS

Characteristics	All (%)	Discovery set (n=212)			Validation set (n=272)		
		High risk	Low risk	P value	High risk	Low risk	P value
Total population	484 (100)	89 (42.0)	123 (58.0)		93 (34.2)	179 (65.8)	
Age (months)				0.084			0.029
<18	228 (100)	30 (34.9)	56 (65.1)		40 (28.2)	102 (71.8)	
≥18	256 (100)	59 (46.8)	67 (53.2)		53 (40.8)	77 (59.2)	
MYCN status				0.047			0.001
Amplified	89 (100)	20 (57.1)	15 (42.9)		29 (53.7)	25 (46.3)	
Non-amplified	395 (100)	69 (39.0)	108 (62.0)		64 (29.4)	154 (70.6)	
INSS*				0.012			0.198
Early	173 (100)	19 (29.2)	46 (70.8)		32 (29.6)	76 (70.3)	
Advanced	331 (100)	70 (47.6)	77 (52.4)		61 (37.2)	103 (62.8)	
Sex				0.362			
Female		30 (38.0)	49 (62.0)				
Male		59 (44.4)	74 (55.6)				
Tissue sample origins				0.850			
Primary		81 (42.2)	111 (57.8)				
Metastatic		8 (40.0)	12 (60.0)				
Preoperative chemotherapy				0.022			
With		38 (52.8)	34 (47.2)				
Without		51 (36.4)	89 (63.6)				
COG				0.085			
High risk		37 (34.6)	70 (65.4)				
Non-high risk		25 (23.8)	80 (76.2)				
Grade				0.498			
Undifferentiated or poorly differentiated		37 (26.8)	101 (73.2)				
Differentiated		24 (33.3)	48 (66.7)				
NA		1	1				
MKI				0.238			
High		6 (18.2)	27 (81.8)				
Intermediate		11 (39.3)	17 (60.7)				
Low		40 (28.8)	99 (71.2)				
NA		5	7				

*Early indicates INSS stage 1, 2, and 4s ; Advanced indicates INSS stage 3 and 4.
COG, Children's Oncology Group; ICS, immune checkpoint-based signature; INSS, the International Neuroblastoma Staging System; MKI, Mitosis-Karyorrhexis Index; NA, not available; NB, neuroblastoma.

Statistical analysis

The primary and secondary outcomes were OS and event-free survival (EFS), respectively, as identified through the medical records. OS was calculated from the date of cancer diagnosis to the date of death from any cause. EFS was determined from the date of cancer diagnosis to the first occurrence of any event (ie, relapse at any site, progressive disease, second malignancy or death).

The correlations between the ICS and clinical variables were analyzed using a χ^2 test or Fisher's exact test. We used Kaplan-Meier curves with a log-rank test method as implemented in the survival R package to compare the differences in OS and EFS between the patients with high and low expression of all seven immune checkpoints and ICS. The HRs with 95% CIs were first calculated using a univariate Cox regression analysis to show the associations between different prognostic indicators, including clinical features and the ICS, and the risk of death or any event (relapse/metastasis/death). A multivariate Cox regression analysis with backwards stepwise selection was then used to test the prognostic roles of these different factors, mutually adjusted for one another. Variables reaching $p<0.05$ in the univariate analysis were included in Cox proportional hazards regression models. Finally, we calculated Youden's index for each nomogram to find their optimal features to achieve minimum false positive

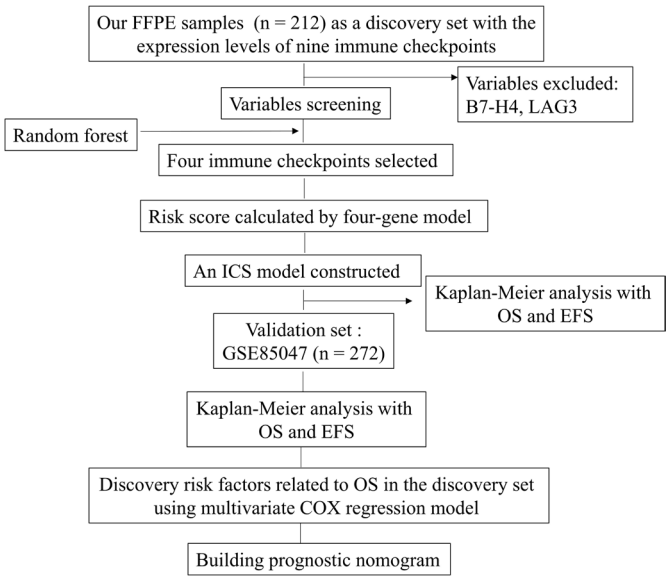

Figure 1 Workflow chart of the data enrollment and analysis for developing a prognostic model with the most common immune checkpoints. EFS, event-free survival; FFPE, formalin-fixed, paraffin-embedded; ICS, immune checkpoint-based signature; LAG3, lymphocyte activation gene 3; OS, overall survival.

rate and the model performance was evaluated by the area under the curve (AUC) using a receiver operating characteristic (ROC) curve and decision curve analysis (DCA).

The statistical analyses were performed using R (V.4.1.2), Stata V.15.1 (Texas, USA) and GraphPad Prism (V.8.0.1, San Diego, California, USA). All statistical tests were two-sided and considered significant when the p value was less than 0.05.

RESULTS

Patient characteristics

Figure 1 shows the study workflow. The 1-year, 3-year and 5-year OS rates in the discovery set were 93.7% (89.5%–96.3%), 78.9% (72.1%–84.2%) and 68.1% (59.1%–75.5%), respectively. In addition, 192 tissue samples from primary tumor, such as thoracic, adrenal gland and retroperitoneal locations, and 20 tissue samples from metastatic tumors, including liver, spinal and brain sites, were evaluated. Among the NB patients, 140 received surgery first, followed by postoperative chemotherapy, and in the remainder, 72 cases received preoperative chemotherapy first, followed by surgery and postoperative chemotherapy (online supplemental table S1). Detailed information on OS and EFS is shown in online supplemental table S2. The median follow-up time was 1033 days (IQR 581–1543) for the NB patients in the discovery set and 1287 days (IQR 451–2436) for those in the validation set.

Expression of immune checkpoints

To evaluate the biological and clinical significance of 9 immune checkpoints in NB, we carried out an IHC analysis of 212 NB FFPE samples. Representative images of IHC staining and the corresponding digital deconvolution of the seven immune checkpoints in the discovery set are shown in online supplemental figure S4. The expression of the seven immune checkpoints and the median number detected in the NB tissue blocks are summarized in online supplemental figure S5A. The highest expression was found for PD-L1 (median: 622.7/mm^2, 95% CI: 525.8 to 757.9), followed by IDO1 (median: 465.4/mm^2, 95% CI: 394.2 to 538.3), B7-H3 (median: 337.5/mm^2, 95% CI: 229.5 to 483.3), VISTA (median: 316.9/mm^2, 95% CI: 275.1 to 357.3), TIM-3 (median: 216.9/mm^2, 95% CI: 186.1 to 265.0), ICOS (median: 173.1/mm^2, 95% CI: 149.8 to 204.6) and OX40 (median: 53.3/mm^2, 95% CI: 41.9 to 64.6).

Subsequently, all data in the two datasets were normalized and transformed into log2 values of z scores for further analysis. Then, we used UpSet plots to evaluate the high coexpression of immune checkpoints in the NB patients in the discovery and validation sets (online supplemental figure S5Band C). In the discovery set, the most common coexpression patterns were PD-L1+VISTA +ICOS + IDO1 + TIM-3 + OX40 + B7 H3 and PD-L1+IDO1, occurring in 3.8% of the patients (8 of 212), whereas PD-L1+VISTA +ICOS + IDO1 +TIM-3 was observed in 16.9% of the patients (46 of 272) in the validation set. It suggests that these costimulatory signals might have a synergistic effect and a combination of ICIs might be useful to improve the clinical outcome of NB patients. More studies are needed for confirmation.

Prognostic values of individual immune checkpoints

Next, we explored the prognostic value of each individual immune checkpoint (PD-L1, IDO1, B7-H3, VISTA, TIM-3, ICOS and OX40) in NB patients. In the discovery set, high expression of B7-H3, OX40 or VISTA was associated with poor OS and EFS (OS, p<0.05, figure 2B, E and F; EFS, p<0.05, figure 2I, L and M). Interestingly, we found that the NB patients with high expression of TIM-3 had poor OS but not EFS in the discovery set (p=0.039, figure 2C; p=0.083, figure 2J). However, PD-L1, ICOS and IDO1 expressions were not significantly associated with OS, as well as EFS (figure 2A, D, H, G, K and N). In contrast, high expression of PD-L1, TIM-3 or ICOS was associated with favorable OS and EFS, whereas high expression of B7-H3 was associated with poor OS and EFS in the validation set (p<0.05, online supplemental figure S6).

ICS construction and its association with clinical outcomes

To better understand the joint prognostic value of these immune checkpoints, we constructed an ICS model comprizing four immune checkpoints using a random forest model, namely, OX40, B7-H3, TIM-3 and ICOS, which were associated with poor OS in the discovery set (online supplemental figure S2). To identify the expression consistency of four immune checkpoints, we compared the expression profile of primary tumors to metastatic tumors, as well as in tumors first treated with

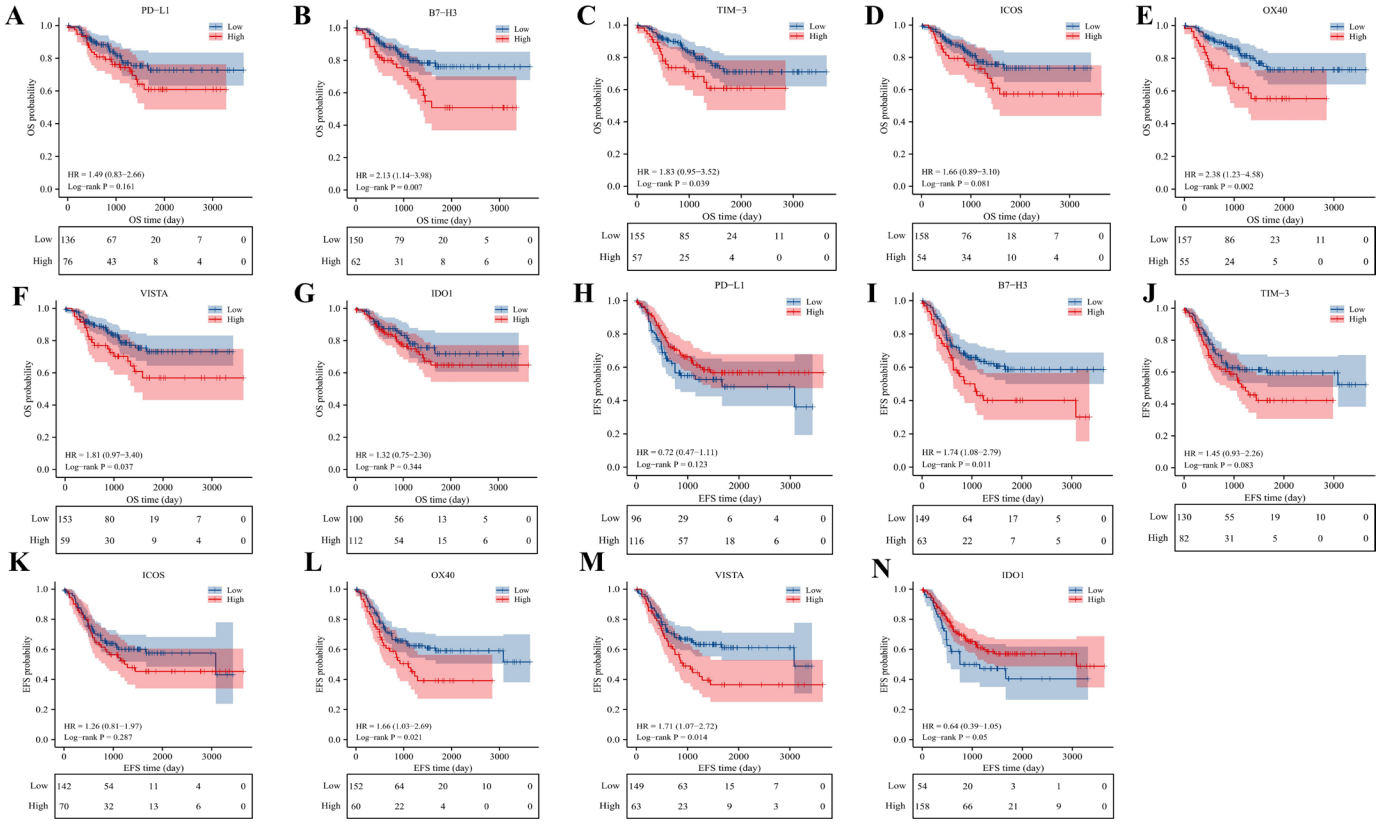

Figure 2 Kaplan-Meier survival analysis of PD-L1, B7-H3, TIM-3, ICOS, OX40, VISTA and IDO1 expression in NB patients in the discovery set (n=212). Survival curves were generated according to the high and low expression of PD-L1, B7-H3, TIM-3, ICOS, OX40, VISTA and IDO1 (OS: (A–G); EFS: (H–N). P values were calculated by the log-rank test. EFS, event-free survival; ICOS, inducible costimulatory molecule; IDO1, indoleamine-pyrrole 2,3-dioxygenase 1; NB, neuroblastoma; OS, overall survival; OX40, costimulatory molecule 40; PD-L1, programmed death ligand 1; TIM-3, T-cell immunoglobulin and mucin domain containing-3.

surgery and preoperative chemo strategies (online supplemental figure S7A and 8). Subsequently, the derived ICS value was also compared (online supplemental figure S7C and D). The result was shown that the OX40 expression was significantly higher in the preoperative chemo tissue samples than in tumors first treated with surgery, which contributed to high value of the ICS.

Next, it was observed that the survival time of the NB patients in the discovery set obviously decreased with increasing risk scores, accompanying the changes in the expression of the four immune checkpoints (online supplemental figure S8). Accordingly, the NB patients were divided into high-risk and low-risk groups based on the cut-off value of the risk score. The high-risk group had shorter OS than the low-risk group in the discovery set (HR 15.91, 95% CI 8.87 to 28.55, figure 3A). Similarly, the NB patients with high risk also had a worse EFS than those with low risk in the discovery set (HR 4.30, 95% CI 2.80 to 6.62, figure 3B). Furthermore, we plotted ROC curves and found that the AUCs with 95% CIs were 0.900 (0.847 to 0.953), 0.836 (0.765 to 0.906) and 0.852 (0.764 to 0.941) for predicting the 1-year, 3-year and 5-year OS rates in the discovery set, respectively. (figure 3C). These results suggest that the ICS has good performance in predicting the OS of NB patients.

Validation of the ICS

To validate whether the ICS has similar prognostic value in different populations, we analyzed the ICS in the validation set (n=272). The patients in the high-risk group had a shorter OS than those in the low-risk group (HR 2.62, 95% CI 1.58 to 4.34, figure 3D) and had a worse EFS in the validation set (HR 2.18, 95% CI 1.42 to 3.35, figure 3E). Moreover, we plotted ROC curves, and the AUCs with 95% CIs were 0.702 (0.597 to 0.807), 0.668 (0.590 to 0.746) and 0.665 (0.583 to 0.746) for predicting the 1-year, 3-year and 5-year OS rates, respectively (figure 3F).

Additionally, we performed univariate and multivariate analyses of all NB patients in the discovery set to determine the independent risk factors for OS among the ICS and clinicopathological features. Our results show that the ICS and age were significantly associated with OS and EFS in NB patients in the discovery set (table 2), and this finding was confirmed in the validation set (online supplemental figure S9).

Prediction model combining the ICS and age

It is well established in the guidelines that the age of NB patients should be used to guide treatment and predict patient outcomes,[1] but its accuracy is limited due to tumor

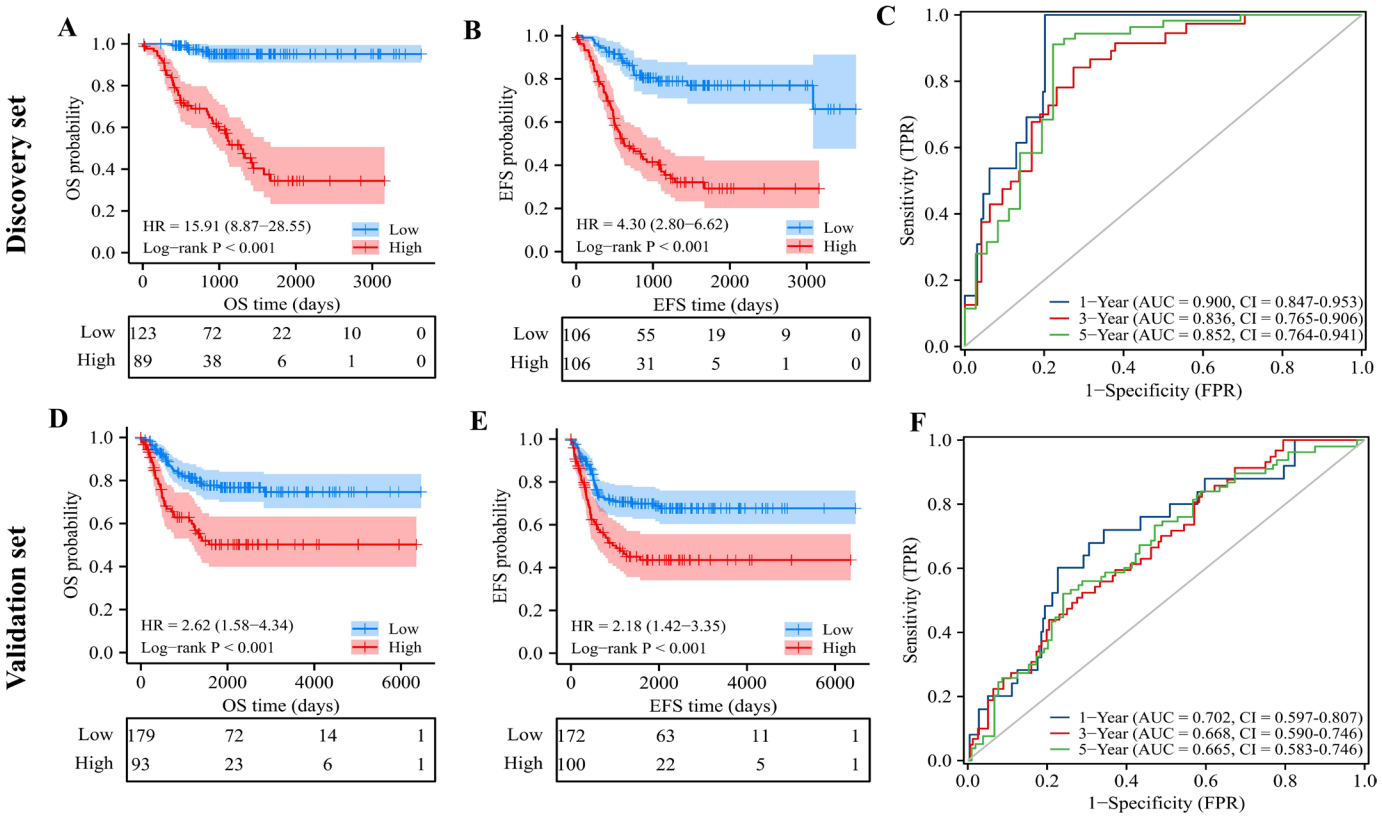

Figure 3 Kaplan-Meier survival and time-dependent ROC curve analyses based on the risk score predicted by the ICS. NB patients were divided into high-risk and low-risk groups according to their risk scores in the discovery set (n=212) and validation set (n=272). There were significant differences in the OS (A,D) and EFS (B,E) probability between the two groups in the discovery and validation sets. The threshold for grouping was based on the principle of a minimum p value of OS probability. According to the AUC of the time-dependent ROC curve of the risk score of the ICS in the discovery set (C) and the validation set (F), good performance of the prediction ability for 1-year, 3-year and 5-year OS was observed. AUC, area under the curve; EFS, event-free survival; FPR, false positive rate; ICS, immune checkpoint-based signature; NB, neuroblastoma; OS, overall survival; ROC, receiver operating characteristic; TPR, true positive rate.

heterogeneity, and age needs to be supplemented with additional molecular indicators. Therefore, we established a more sensitive model based on the multivariate Cox regression analysis, nomogram A, which combined the ICS and age to estimate the survival of NB patients in the discovery set (figure 4A). In addition, we established nomogram B using only age in the discovery set. Harrell's concordance index of nomogram A compared with nomogram B in predicting OS was 0.848 (95% CI 0.820 to 0.876) vs 0.679 (95% CI 0.652 to 0.705) in the discovery set, and this finding was confirmed in the validation set (0.765 (95% CI 0.735 to 0.794) vs 0.697 (95% CI 0.670 to 0.724)).

Meanwhile, the calibration plot of nomogram A for the probability of 1-year OS (figure 4B), 3-year OS (figure 4C) or 5-year OS (figure 4D) showed optimal agreement between the prediction by the nomogram and the actual events in the discovery set. Furthermore, the combination of the ICS and age showed significantly better prognostic value than age alone in predicting the 1-year, 3-year and 5-year OS (AUROC 0.891 (95% CI 0.797 to 0.985) vs 0.675 (95% CI 0.592 to 0.758), p<0.0001, figure 4E; 0.875 (95% CI 0.817 to 0.933) vs 0.701 (95% CI 0.645 to 0.758), p<0.0001, figure 4F; 0.898 (95% CI 0.851 to 0.940) vs 0.724 (95% CI 0.673 to 0.775), figure 4G). The similar result was conformed in the validation set (online supplemental figure S9). We further comprehensively compared the sensitivity, specificity and accuracy and Youden index of nomograms A and B for predicting OS in the discovery and validation sets (online supplemental table S4), suggesting that the addition of ICS to nomogram A significantly enhanced its accuracy compared with that of nomogram B (p<0.001). The DCA analysis showed similar results (online supplemental figure S10). Overall, combining of ICS and age might increase the predictive power for patient survival.

DISCUSSION

In this study, we first determined the expression of nine immune checkpoints using digital pathology and assessed their prognostic significance in NB patients. Then, we constructed a novel prognostic model, the ICS, based on the expression of four immune checkpoints. Their combination had a superior ability to predict the survival of NB patients relative to the individual immune checkpoints in the discovery set. Then, we confirmed its value in the validation set. In addition, age is an important factor in predicting patient survival in NB. Therefore, we developed a nomogram

Table 2 Cox regression analysis of factors associated with survival in all NB patients from the discovery set

Factors	Univariate		Multivariate	
	HR (95% CI)	P value	HR (95% CI)	P value
OS				
Age, months (≥18 vs <18)	12.48 (3.87 to 40.22)	**<0.001**	6.17 (1.78 to 21.29)	**0.004**
INSS (advanced vs early)	6.10 (2.19 to 17.00)	**<0.001**	1.95 (0.65 to 5.84)	0.231
MYCN (amplified vs non-amplified)	2.47 (1.30 to 4.68)	**0.006**	1.29 (0.65 to 2.57)	0.457
Grade (undifferentiated or poorly vs well)	1.90 (1.08 to 3.35)	**0.026**	1.69 (0.93 to 3.07)	0.085
MKI (high vs non-high)	1.69 (0.60 to 4.73)	0.313		
ICS (high vs low)	1.21 (1.15 to 1.27)	**<0.001**	1.18 (1.12 to 1.25)	**<0.001**
EFS				
Age, months (≥18 vs <18)	3.97 (2.26 to 6.95)	**<0.001**	2.19 (1.20 to 4.00)	**0.010**
INSS (advanced vs early)	6.71 (3.09 to 14.57)	**<0.001**	4.01 (1.75 to 9.17)	**0.001**
MYCN (amplified vs non-amplified)	1.94 (1.16 to 3.24)	**0.011**	1.04 (0.62 to 1.76)	0.879
Grade (undifferentiated or poorly vs well)	1.30 (0.84 to 2.01)	0.225		
MKI (high vs non-high)	1.06 (0.56 to 2.02)	0.840		
ICS (high vs low)	1.14 (1.10 to 1.19)	**<0.001**	1.11 (1.07 to 1.16)	**<0.001**

Statistically significant p values are shown in bold.
. EFS, event-free survival; ICS, immune checkpoint-based signature; INSS, the International Neuroblastoma Staging System; NB, neuroblastoma; OS, overall survival.

combining the ICS and age, which demonstrated a better prognostic value than age alone for NB patients. To the best of our knowledge, this study is the first to comprehensively evaluate the most common and immunologic variables using digital pathology and construct an ICS prognostic model for NB patients. Our study provides proof of principle that the ICS could serve as a selection tool for immunotherapy targets for NB patients.

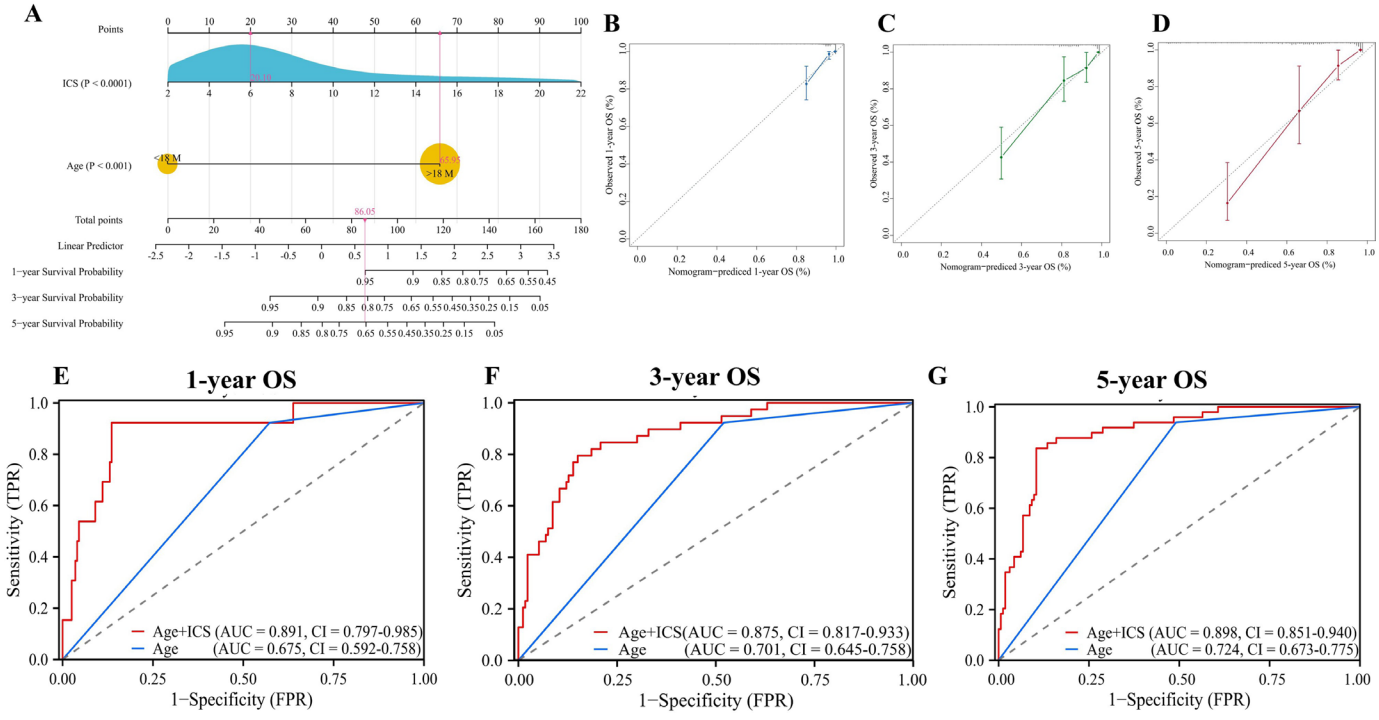

Figure 4 Nomogram, calibration plots and comparisons of the sensitivity and specificity for predicting 1-year, 3-year and 5-year OS in the discovery set. (A) Nomogram A, including ICS and age; (B–D) Calibration plots for predicting 1-year, 3-year and 5-year OS; ROC curves of nomograms A and B as predictors of 1-year OS (E), 3-year OS (F) and 5-year OS (G). AUC, area under the curve; ICS, immune checkpoint-based signature; NB, neuroblastoma; OS, overall survival; ROC, receiver operating characteristic; TPR, true positive rate; FPR, false positive rate.

The four immune checkpoints, B7-H3, TIM-3, ICOS and OX40, were selected for inclusion in the ICS for predicting NB patient survival. B7-H3 has been shown to lead to a protumorigenic or non-immunologic protumorigenic functions, such as promoting migration /invasion, angiogenesis and endothelial-to-mesenchymal transition in malignant tissues,[16] and therefore, its high expression is associated with poor outcomes in various cancers.[17] In NB, it was shown that B7-H3 downregulates natural killer cytotoxicity, providing a mechanism of escape from the immune response,[18] and it could be speculated that high B7-H3 expression could concomitantly result in a poor prognosis. In particular, Tian *et al* identified an optimized bicistronic chimeric antigen targeting B7-H3 with high and heterogeneous expression in NB.[19] These observations are consistent with our data demonstrating that high expression level of B7-H3 was significantly associated with unfavorable OS and EFS in the training and validation cohorts. Accordingly, these phenomena could explain why NB patients with high B7-H3 expression have significantly inferior OS and EFS, and they also suggest B7-H3 is an encouraging target for immunotherapy.

TIM-3 is predominantly expressed by myeloid cells and is coexpressed on exhausted T cells along with PD-1. Dixon *et al* proposed that the expression of TIM-3 in the TME is considered a cardinal sign of T-cell dysfunction; for instance, genetic loss of TIM-3 in intrastromal dendritic cells promotes antitumor immunity, whereas its loss in T cells does not alter tumorigenesis.[20] TIM-3 blockade can promote CD8 T-cell-dependent responses to paclitaxel treatment in models of breast cancer,[21] whereas a study from TCGA large cohort showed that TIM-3 was a favorable prognosis in breast cancer.[22] Again, a previous study revealed that higher expression of TIM-3 was significantly associated with shorter OS in hepatocellular carcinoma.[23] Consistently, TIM-3 expression was identified to be a risk factor for worse OS but not for disease-free survival in 9491 TCGA patients. In NB, Pei *et al* have demonstrated that the ratio of exhausted T cells was increased with the characteristics of upregulated PD-1 and TIM-3,[24] suggesting that the high expression of TIM-3 could impair T-cell functions and result in poor survival. Concordant with these investigations, we found that TIM-3 was expressed in tumor-associated immune cells of NB tissues and that high expression of TIM-3 was a significant risk factor for a shorter OS, as well as a marginally significant factor for a poor EFS in the discovery set. On the contrary, the high expression of TIM-3 was associated with satisfying OS and EFS in the validation set, presumably that different expression levels of TIM-3, mRNA and protein, attribute to this. As we all know, gene expression is complex and involves multiple process such as transcription, translation and the turnovers of mRNAs and proteins. The consistency of mRNAs and protein levels is somewhat low, modest or high and mainly depends on the considerations as indicated above. A previous study has been demonstrated that the consistent result that TIM-3 high expression related to worse survival in TCGA data using the IHC data and gene expression data was obtained.[22] Therefore, the relationship and underlying mechanisms behind this phenomenon need to be further explored.

Abnormalities of ICOS, which is abundantly and commonly expressed in the activated and mature T cells, lead to a range of pathological dysfunctions, such as immunodeficiency and malignant tumors. However, the role of ICOS seems to vary among various cancer. For example, gastric cancer patients with abundant ICOS+Foxp3+ TILs had advanced stages and shorter recurrence-free survival,[25] and high expression of ICOS was associated with an advanced clinical stage and poor OS among patients with cutaneous T-cell lymphoma.[26] In contrast, ICOS enhances the activation of CD4 and CD8 effector T cells to exert an antitumor function in colorectal cancer.[27 28] In this study, we found that high expression of ICOS mRNA, but not the protein level, is a protective factor for OS and EFS in NB patients, but this requires further verification in a larger patient cohort.

The OX40–OX40L pathway provides crucial costimulatory signals for CD4 T-cell responses and, more importantly, impairs Treg suppressive ability, presumably through direct inhibition of Foxp3 expression. On the one hand, OX40 expression has been observed in all TILs, such as natural killer T cells and neutrophils, and it is associated with favorable survival in non-small cell lung cancer.[7] On the other hand, a recent study demonstrated that OX40 expression in nasopharyngeal carcinoma patients was not significantly associated with survival.[29] As expected, the OX40 effect on anti-Tregs could depend on the TME, notably the tumor bed.[30] In line with this concept, we detected OX40 expression in tumor-associated immune cells of NB, and patients with high OX40 expression had inferior OS and EFS. Interestingly, for the timing of tumor tissues obtained, we observed OX40 expression increased in NB patients who received preoperative chemotherapy compared with those patients with receiving surgery first. Chemotherapy is the main treatment in NB either before surgery (preoperative chemotherapy) or after surgery (postoperative chemotherapy), especially when cancers spread too far to be removed completely by surgery for NB patients who generally had a poor prognosis. Li *et al* reported that the expression level of OX40 in serum and tumor tissues of lung carcinoma was significantly upregulated under stress conditions such as receiving chemotherapy, implying chemoresistance facilitation through inhibiting tumor cell apoptosis.[31] Accordingly, it was assuming that OX40 could induce to some extent chemoresistance in NB, which showed rational for the combination of chemotherapy with ICIs. D'Errico *et al* have reviewed that modulating immune costimulating signaling (such as OX40) and immune checkpoints are the most prospective regimens in cancer treatment.[32] Together, these could explain why the high expression of OX40 resulted in worse OS and EFS of NB patients, potentially due to inducing chemoresistance. The exact mechanisms will be further studied, and in vivo and in vitro studies are

required to confirm this harmful role in NB patients. Overall, it is speculated that these four immune checkpoints are important for predicting patient outcomes and providing potential immune targets in NB.

Digital pathology is in widespread use, providing a tool for more automatic and objective quantification of full-view slides.[33] Wang *et al* used digital pathology to evaluate the expression of immune checkpoints and presented an ICS based on five immune checkpoint features for nasopharyngeal carcinoma tumor cells and tumor-associated immune cells and found this ICS could predict patient survival.[29] Regarding the expression pattern of immune checkpoints as indicated above, there were different status existed across cancer types. The US food and drug administration-approved test confirmed that the PD-L1 combined positive score (>1%) was used as a criterion to predict the response rate of metastatic head and neck squamous cell carcinoma, advanced esophageal carcinoma, advanced cervical cancer and triple-negative breast cancer.[34] Taken together, PD-L1 expression in both tumor cells and tumor-associated immune cells are inferred to be effective as a hall marker in immune therapy in most cancers. Therefore, we also defined the expression of PD-L1 in combined areas, while the remaining genes were identified in tumor cells or tumor-associated immune cells to predict the patient outcomes.

We found that a model combining ICS and age had good performance for prognostication since these two variables were independent risk factors for OS and EFS in multivariate analysis in both the training and validation cohorts in our study. In contrast, INSS and MYCN amplification were significant predictors of OS and EFS in only the validation cohort. A previous study showed that age, especially a median of 18 months, is an important factor for NB risk assessment and treatment decision-making.[35] In clinical practice, NB patient's age is defined as the date of diagnosis based on the pathology review and it is easily recorded and obtained from medical records. In addition, the confirmation of MYCN amplification followed by metaphases is detected by fluorescence in situ hybridization and observed in approximately 20% of NB cases, and it is associated with a worse prognosis,[36] while another recent study showed that MYCN mRNA levels are better than MYCN amplification in predicting prognosis in NB.[37] The INSS uses tumor location, lymph node status, bone marrow metastasis and imaging studies to detect metastasis. Additionally, Ray *et al* have reported that sensitivity, specificity, accuracy, Youden index as well as ROC analysis would be focused together to assess the ability of survival risk of a biomarker.[38] In this case, when testing for sensitivity of nomogram A and B, we recommend applying integrated analytic methods to assess a potential application in predicting prognosis. The results suggest a nomogram composed of an ICS and age might be easily obtained and allow for more accurate classification of NB patients at different risks.

NB is generally characterized by low immunogenicity due to its lower tumor mutation burden and lower infiltration of immune cells,[39] impeding their effective engagement during immunotherapy.[40] However, it has been recently noted that cold tumors featuring lower densities of immune cells should be treated with ICIs in combination with priming therapy, which may enhance T-cell responses to convert an immune cold tumor to an immune hot tumor.[41] Thus, a different or more extensive biomarker should be identified for the successful implementation of novel immunotherapies in NB patients to improve their survival.

There were some limitations of this study, which suffers from different bias, such as its retrospective nature, its relatively small number of cases and the mixed used of tumor tissues receiving or not receiving preoperative chemotherapy. We did not confirm the ICS model as a tool for clinical practice in a wide cohort of NB patients, which would need to be addressed by independent cohort sources to validate our findings.

Collectively, our data reveal that the aberrant expression of immune checkpoints is a prognostic factor in NB patients. Additionally, the ICS based on the expression levels of four immune checkpoints could guide NB patients' risk stratification into different prognostic profiles. The combination of the ICS and age is a more robust model for predicting clinical outcomes. Altogether, these findings might provide clues for the novel implementation of immunotherapy in NB patients.

Author affiliations
[1]Department of Pathology, Guangzhou Women and Children's Medical Center, Guangzhou Medical University, Guangdong Provincial Clinical Research Center for Child Health, National Children's Medical Center for South Central Region, Guangzhou, China
[2]Molecular Diagnosis and Gene Testing Center, The First Affiliated Hospital, Sun Yat-sen University, Guangzhou, China
[3]Department of General Surgery, Southern Medical University Nanfang Hospital, Guangzhou, China
[4]Bio-totem Pte. Ltd, Foshan, China
[5]Guangzhou Institute of Paediatrics, Guangzhou Women and Children's Medical Center, Guangzhou Medical University, Guangdong Provincial Clinical Research Center for Child Health,Guangdong Provincial Key Laboratory of Research in Structural Birth Defect Disease, National Children's Medical Center for South Central Region, Guangzhou, China
[6]Department of Molecular Diagnostics, Sun Yat-sen University Cancer Center, State Key Laboratory of Oncology in South China; Collaborative Innovation Center for Cancer Medicine, Guangzhou, China
[7]Department of Thoracic Surgery, Guangzhou Women and Children's Medical Center, Guangzhou Medical University, Guangzhou, China
[8]Guangdong Provincial Key Laboratory of Malignant Tumour Epigenetics and Gene Regulation, Cellular & Molecular Diagnostics Center, Sun Yat-Sen Memorial Hospital, Guangzhou, China
[9]Department of Experimental Research, State Key Laboratory of Oncology in Southern China, Collaborative Innovation Center for Cancer Medicine, Guangdong Key Laboratory of Nasopharyngeal Carcinoma Diagnosis and Therapy, Sun Yat-sen University Cancer Center, Guangzhou, China
[10]Department of Pathology, The First Affiliated Hospital, Sun Yat-sen University, Guangzhou, China
[11]State Key Laboratory of Oncology in South China, Sun Yat-sen University Cancer Center; Collaborative Innovation Center of Cancer Medicine, Guangzhou, China

Acknowledgements We thank senior engineer Wei Wang (Cellsvision (Guangzhou) Medical Technology, Guangzhou, China) for the professional image scanning for this study. We also thank American Journal Experts for the English polishing service used in this manuscript.

Contributors H-YW and LZ: Conception and design. LZ, S-HL, KC, HX and L-JQ: Implementation. LZ and KC: Review of immunohistochemistry slides. S-YX: Computational pathology analysis. H-YW, LZ, Y-QL and S-YX: Analysis and interpretation of the data. FW, LD, SF, S-HL, F-HW, LL, RW and LM: Clinical data retrieval. H-YW, LZ, S-YX and NL: Manuscript drafting. H-YW: Guarantor. All authors were involved in the writing of the manuscript at the draft and all revision stages and read and approved the final version.

Funding This work was partially supported by the start-up program of Guangzhou Women and Children's Medical Center (No. 3001151-04), the Basic Research Project (Dengfeng Hospital) jointly funded by municipal schools/hospitals (No. 202201020642) and Plan on enhancing scientific research in GMU.

Competing interests None declared.

Patient consent for publication Not applicable.

Ethics approval Prior to using the human tissue formalin-fixed, paraffin-embedded samples and clinical data of the investigated patients for research purposes, written informed consent was obtained from the parents of all patients, and approval was obtained from the Institute Research Ethics Committee of Guangzhou Women and Children's Medical Center ((2021)078A01).

Provenance and peer review Not commissioned; externally peer reviewed.

Data availability statement Data are available upon reasonable request. All data relevant to the study are included in the article or uploaded as online supplemental information.

ORCID iDs
Hui Xu http://orcid.org/0000-0002-4443-4404
Hai-Yun Wang http://orcid.org/0000-0002-1385-0827

REFERENCES

1 Irwin MS, Naranjo A, Zhang FF, *et al*. Revised neuroblastoma risk classification system: a report from the children's Oncology Group. *JCO* 2021;39:3229–41.
2 Maris JM. Recent advances in neuroblastoma. *N Engl J Med* 2010;362:2202–11.
3 Matthay KK, Maris JM, Schleiermacher G, *et al*. Neuroblastoma. *Nat Rev Dis Primers* 2016;2:16078.
4 Passaro A, Brahmer J, Antonia S, *et al*. Managing resistance to immune checkpoint inhibitors in lung cancer: treatment and novel strategies. *JCO* 2022;40:598–610.
5 Burugu S, Gao D, Leung S, *et al*. LAG-3+ tumor infiltrating lymphocytes in breast cancer: clinical correlates and association with PD-1/PD-L1+ tumors. *Ann Oncol* 2017;28:2977–84.
6 Burugu S, Dancsok AR, Nielsen TO. Emerging targets in cancer immunotherapy. *Semin Cancer Biol* 2018;52:39–52.
7 Massarelli E, Lam VK, Parra ER, *et al*. High ox-40 expression in the tumor immune infiltrate is a favorable prognostic factor of overall survival in non-small cell lung cancer. *J Immunother Cancer* 2019;7:351.
8 Girardi DM, Niglio SA, Mortazavi A, *et al*. Cabozantinib plus nivolumab phase I expansion study in patients with metastatic urothelial carcinoma refractory to immune checkpoint inhibitor therapy. *Clin Cancer Res* 2022;28:1353–62.
9 Wienke J, Dierselhuis MP, Tytgat GAM, *et al*. The immune landscape of neuroblastoma: challenges and opportunities for novel therapeutic strategies in pediatric oncology. *Eur J Cancer* 2021;144:123–50.
10 He X, Qin C, Zhao Y, *et al*. Gene signatures associated with genomic aberrations predict prognosis in neuroblastoma. *Cancer Commun (Lond)* 2020;40:105–18.
11 Brodeur GM, Pritchard J, Berthold F, *et al*. Revisions of the International criteria for neuroblastoma diagnosis, staging, and response to treatment. *J Clin Oncol* 1993;11:1466–77.
12 McShane LM, Altman DG, Sauerbrei W, *et al*. Reporting recommendations for tumor marker prognostic studies (REMARK). *J Natl Cancer Inst* 2005;97:1180–4.
13 Qiao H, Tan X-R, Li H, *et al*. Association of intratumoral microbiota with prognosis in patients with nasopharyngeal carcinoma from 2 hospitals in China. *JAMA Oncol* 2022;8:1301–9.
14 Loughrey MB, Bankhead P, Coleman HG, *et al*. Validation of the systematic scoring of immunohistochemically stained tumour tissue microarrays using qupath digital image analysis. *Histopathology* 2018;73:327–38.
15 Devereaux PJ, Chan MTV, Alonso-Coello P, *et al*. Association between postoperative troponin levels and 30-day mortality among patients undergoing noncardiac surgery. *JAMA* 2012;307:2295–304.
16 Kontos F, Michelakos T, Kurokawa T, *et al*. B7-H3: an attractive target for antibody-based immunotherapy. *Clin Cancer Res* 2021;27:1227–35.
17 Du H, Hirabayashi K, Ahn S, *et al*. Antitumor responses in the absence of toxicity in solid tumors by targeting B7-H3 via chimeric antigen receptor T cells. *Cancer Cell* 2019;35:221–37.
18 Bottino C, Dondero A, Bellora F, *et al*. Natural killer cells and neuroblastoma: tumor recognition, escape mechanisms, and possible novel immunotherapeutic approaches. *Front Immunol* 2014;5:56.
19 Tian M, Cheuk AT, Wei JS, *et al*. An optimized bicistronic chimeric antigen receptor against GPC2 or CD276 overcomes heterogeneous expression in neuroblastoma. *J Clin Invest* 2022;132:e155621.
20 Dixon KO, Tabaka M, Schramm MA, *et al*. Tim-3 restrains anti-tumour immunity by regulating inflammasome activation. *Nature* 2021;595:101–6.
21 de Mingo Pulido Á, Gardner A, Hiebler S, *et al*. Tim-3 regulates cd103+ dendritic cell function and response to chemotherapy in breast cancer. *Cancer Cell* 2018;33:60–74.
22 Zang K, Hui L, Wang M, *et al*. Tim-3 as a prognostic marker and a potential immunotherapy target in human malignant tumors: a meta-analysis and bioinformatics validation. *Front Oncol* 2021;11:579351.
23 Liu F, Liu Y, Chen Z. Tim-3 expression and its role in hepatocellular carcinoma. *J Hematol Oncol* 2018;11:126.
24 Pei M, Chai W, Wang X, *et al*. The transcription factor tox is involved in the regulation of T-cell exhaustion in neuroblastoma. *Immunol Lett* 2022;248:16–25.
25 Nagase H, Takeoka T, Urakawa S, *et al*. Icos (+) FOXP3 (+) tils in gastric cancer are prognostic markers and effector regulatory T cells associated with Helicobacter pylori. *Int J Cancer* 2017;140:686–95.
26 Di Raimondo C, Rubio-Gonzalez B, Palmer J, *et al*. Expression of immune checkpoint molecules programmed death protein 1, programmed death-ligand 1 and inducible T-cell co-stimulator in mycosis fungoides and Sézary syndrome: association with disease stage and clinical outcome. *Br J Dermatol* 2022;187:234–43.
27 Nelson MH, Kundimi S, Bowers JS, *et al*. The inducible costimulator augments tc17 cell responses to self and tumor tissue. *J Immunol* 2015;194:1737–47.
28 Zhang Y, Luo Y, Qin S-L, *et al*. The clinical impact of ICOS signal in colorectal cancer patients. *OncoImmunology* 2016;5:e1141857.
29 Wang Y-Q, Zhang Y, Jiang W, *et al*. Development and validation of an immune checkpoint-based signature to predict prognosis in nasopharyngeal carcinoma using computational pathology analysis. *J Immunother Cancer* 2019;7:298.
30 Aspeslagh S, Postel-Vinay S, Rusakiewicz S, *et al*. Rationale for anti-ox40 cancer immunotherapy. *Eur J Cancer* 2016;52:50–66.
31 Li Y, Chen Y, Miao L, *et al*. Stress-Induced upregulation of TNFSF4 in cancer-associated fibroblast facilitates chemoresistance of lung adenocarcinoma through inhibiting apoptosis of tumor cells. *Cancer Letters* 2021;497:212–20.
32 D'Errico G, Machado HL, Sainz B. A current perspective on cancer immune therapy: step-by-step approach to constructing the magic bullet. *Clin Transl Med* 2017;6:3.
33 Baxi V, Edwards R, Montalto M, *et al*. Digital pathology and artificial intelligence in translational medicine and clinical practice. *Mod Pathol* 2022;35:23–32.
34 Davis AA, Patel VG. The role of PD-L1 expression as a predictive biomarker: an analysis of all US food and drug administration (FDA) approvals of immune checkpoint inhibitors. *J Immunother Cancer* 2019;7:278.
35 Schmidt ML, Lal A, Seeger RC, *et al*. Favorable prognosis for patients 12 to 18 months of age with stage 4 nonamplified MYCN

neuroblastoma: a children's cancer Group study. *J Clin Oncol* 2005;23:6474–80.
36 Seeger RC, Brodeur GM, Sather H, *et al*. Association of multiple copies of the N-myc oncogene with rapid progression of neuroblastomas. *N Engl J Med* 1985;313:1111–6.
37 Chang H-H, Tseng Y-F, Lu M-Y, *et al*. Mycn RNA levels determined by quantitative in situ hybridization is better than MYCN gene dosages in predicting the prognosis of neuroblastoma patients. *Mod Pathol* 2020;33:531–40.
38 Ray P, Le Manach Y, Riou B, *et al*. Statistical evaluation of a biomarker. *Anesthesiology* 2010;112:1023–40.
39 Gröbner SN, Worst BC, Weischenfeldt J, *et al*. Author correction: the landscape of genomic alterations across childhood cancers. *Nature* 2018;559:E10.
40 Galluzzi L, Chan TA, Kroemer G, *et al*. The hallmarks of successful anticancer immunotherapy. *Sci Transl Med* 2018;10:1–14.
41 Bonaventura P, Shekarian T, Alcazer V, *et al*. Cold tumors: a therapeutic challenge for immunotherapy. *Front Immunol* 2019;10:168.

Supplementary Materials

Methods

Antibodies used and immunohistochemistry

The following primary antibodies were used as following: anti-B7-H4 (clone HPA054200, 1:400; Sigma–Aldrich, Ronkonkoma, NY, USA), anti-LAG3 (clone D2G40, 1:100; Cell Signaling Technology, CST, Beverly, Massachusetts), anti-PD-L1 (clone E1L3N, 1:200 dilution; CST), anti-B7-H3 (clone D9M2 L, 1:300; CST), anti-IDO1 (clone D5J4E; 1:400; CST), anti-VISTA (clone D1L2G, 1:500; CST), anti-TIM-3 (clone D5D5R, 1:400; CST), anti-ICOS (clone D1K2T, 1:1600; CST), and anti-OX40 (ab119904, 1:1600; Abcam, Cambridge, UK).

Digital image analysis

The immune checkpoint PD-L1 is expressed by both tumor cells and tumor-associated immune cells and were assessed in combination with both compartments. In contrast, B7-H3 is expressed only by tumor cells whereas IDO1, VISTA, TIM-3, ICOS, and OX40 are expressed by tumor-associated immune cells and were assessed only in the tumor cells or tumor-associated immune cells compartment. B7-H4 and LAG3 were all negative in the tissue samples. All cell nuclei in the tumour bulk were identified in haematoxylin channel images after stain deconvolution [1] using a Mask-RCNN-based instance segmentation model. [2] The positive nuclei were further recognized according to the intensities in the DAB channel image, and the density of the positive nuclei in the tumor bulk was calculated. Based

Zeng L, *et al. J Immunother Cancer* 2023; 11:e005980. doi: 10.1136/jitc-2022-005980

on a computational pathology analysis, the expression of the immune checkpoints was digitally defined and quantified as the number of positive expression in combined areas (per mm^2), including tumor cells and/or tumor-associated immune cells.

Random forest for ICS construction

Random forest is a complex nonlinear model and built using the R package "randomForestSRC 3.1.0. As the number of trees increased, the error rate gradually stabilized between 0.42 and 0.44 (**Supplementary Figure S2A**). We used an ensemble of 177 estimator trees and Gini entropy to evaluate the quality of a split at each code of a tree. The variable performance measures were generated based on the Gini index of the random forest model (**Supplementary Figure S2B**). Eventually, the top four immune checkpoints, OX40, B7-H3, ICOS, and TIM-3, were selected for the model (**Supplementary Figure S2B**). The out-of-bag (OOB) Brier and OOB continuous rank probability score (CRPS) were consistently used to evaluate the prediction accuracy of the model. The OOB Brier and OOB CRPS gradually increased as the OS time increased (**Supplementary Figure S2C and S2D**). **Supplementary Figure S2E** shows a decision tree in the random forest. A nonlinear relationship existed between the four selected genes and mortality (**Supplementary Figure S2F, S2G, S2H and S2I**). The model was constructed using the discovery set of our FFPE cases (n = 212), and then, we grouped the NB patients into low- and high-risk groups based on the ICS scores using a minimum *P* value.

The model was further validated in the GSE85047 dataset. We used the "predict.rfsrc" function of the R package "randomForestSRC" to confirm the prediction value of the ICS in the validation set.

References

1 Ruifrok AC, Katz RL, Johnston DA. Comparison of quantification of histochemical staining by hue-saturation-intensity (HSI) transformation and color-deconvolution. Appl Immunohistochem Mol Morphol 2003; 11: 85-91.

2 Jung H, Lodhi B, Kang J. An automatic nuclei segmentation method based on deep convolutional neural networks for histopathology images. BMC Biomed Eng 2019; 1: 24.

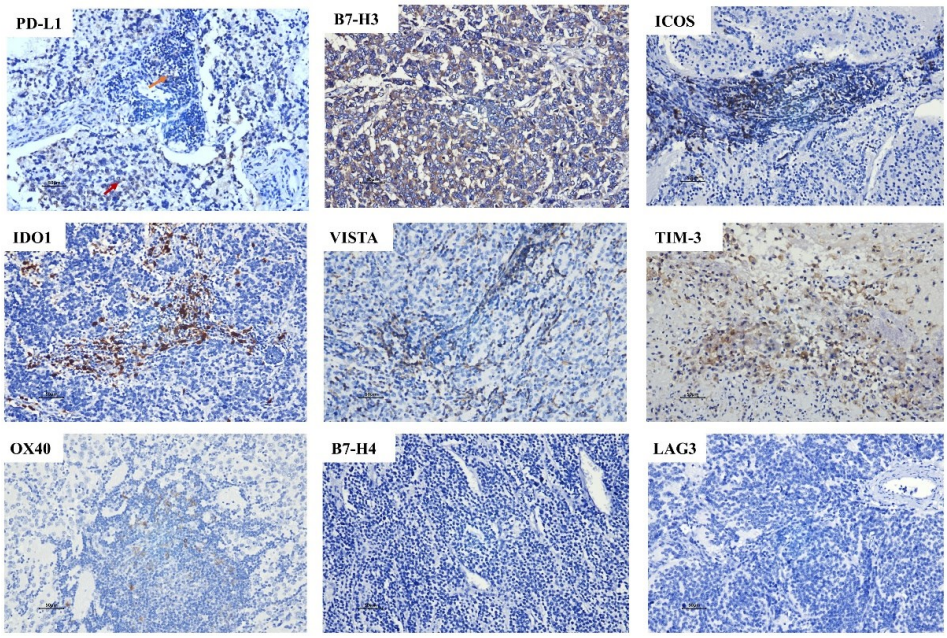

Supplementary Figure S1. Representative images of nine immune checkpoints in NB FFPE samples determined by IHC. The immune checkpoint PD-L1 shows positive expression in both compartments of tumor cells (*dark red arrow indicated*) and tumor-associated immune cells (*orange arrow indicated*), and B7-H3 only in tumor cells; IDO1, VISTA, TIM-3, ICOS, and OX40 are only expressed in tumor-associated immune cells; B7-H4 and LAG3 are not expressed in the NB FFPE samples (original magnification, 200×).

Abbreviations: NB, neuroblastoma; IHC, immunohistochemistry; FFPE, formalin-fixed, paraffin-embedded; PD-L1, programmed death-ligand 1; IDO, indoleamine-pyrrole 2,3-dioxygenase; LAG3, lymphocyte activation gene 3; TIM-3, T cell immunoglobulin and mucin domain containing-3; ICOS, inducible costimulatory molecule; OX40, costimulatory molecule 40.

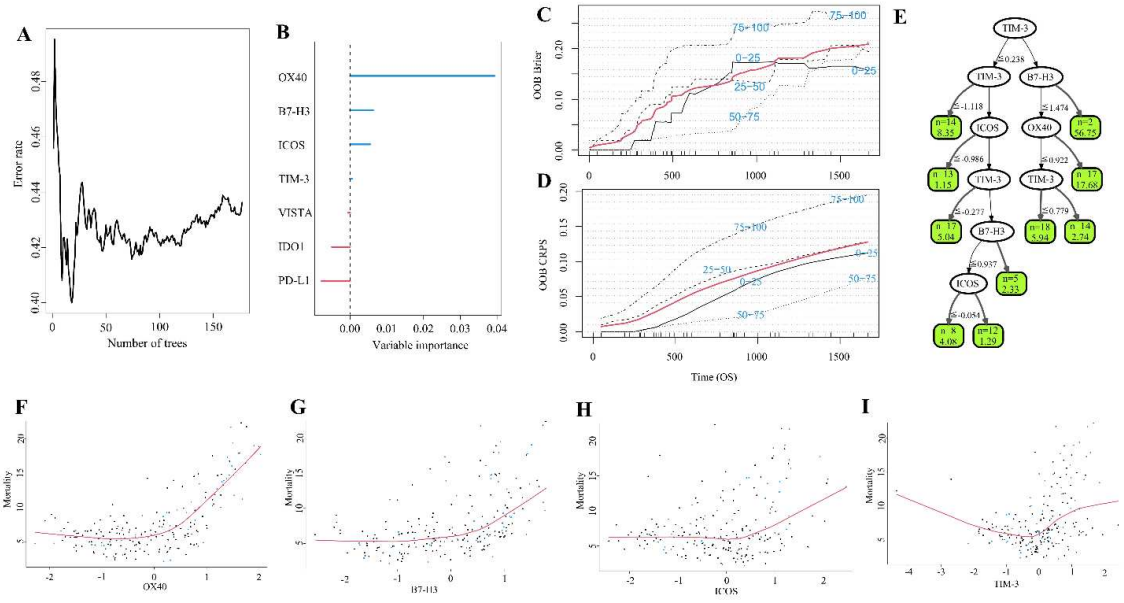

Supplementary Figure S2: Variable selection and construction of the ICS, a classifier comprising four immune checkpoints, using a random forest model in the discovery set (n = 212).

(A) Seven variables were included in the random forest model, and as the number of trees increased, the error rate gradually stabilized between 0.42-0.44. When the parameter "ntree" was set to 177, we calculated the Gini index of these seven variables. Plot (B) shows the importance of seven variables when predicting OS. According to the importance ranking (variable importance > 0), OX40, B7-H3, ICOS and TIM-3 were selected for the model. Since the random forest model cannot be visualized directly, the decision tree was used to indirectly reflect the prediction process of the model. The out-of-bag (OOB) Brier and OOB continuous rank probability score (CRPS) were consistently used to evaluate the prediction accuracy of the model. Plots (C and D) show that the OOB Brier and OOB CRPS gradually increase as the OS time increased. Brier score (0 = perfect, 1 = poor, and 0.25 = guessing) stratified by ensemble mortality. Stratification was performed into 4 groups corresponding to the 0-25, 25-50, 50-75 and 75-100 percentile values of mortality. The red line is the overall (nonstratified) Brier score. CRPS equals the integrated Brier score divided by

time. Plot (E) shows a decision tree in the random forest. A nonlinear relationship exists between the four selected genes, OX40 (F), B7-H3 (G), ICOS (H) and TIM-3 (I), and mortality. Overall, TIM-3 was a protective factor, whereas OX40, B7-H3 and ICOS were risk factors.

Abbreviations: ICS, immune checkpoint-based signature; OOB, out-of-bag; CRPS, continuous rank probability score; TIM-3, T cell immunoglobulin and mucin domain containing-3; ICOS, inducible costimulatory molecule; OX40, costimulatory molecule 40.

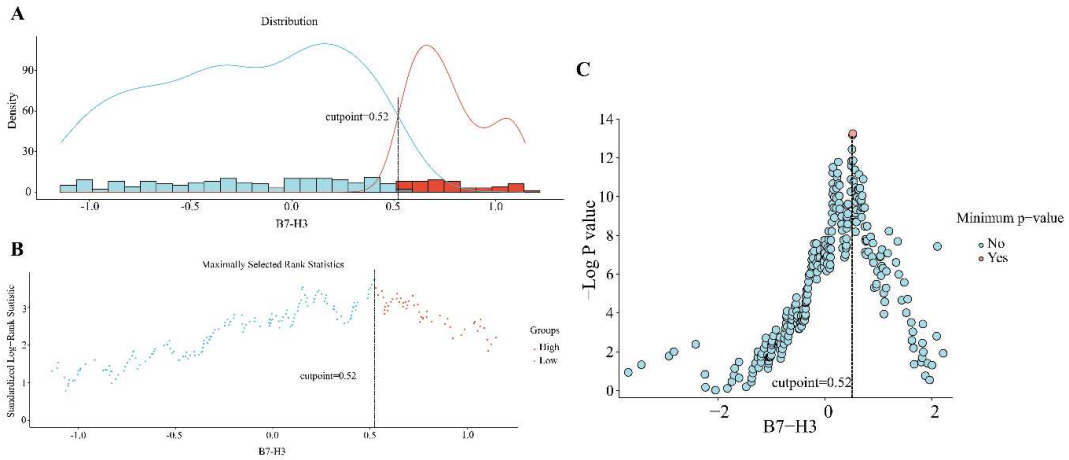

Supplementary Figure S3. An example of the variable grouping, B7-H3, using the minimum *P* value method capable of exploring the prognostic value of variables as much as possible. (A) The distribution of B7-H3 expression with density in the discovery set. (B) Scatter plot showing the relationship between the threshold of B7-H3 and the standard log-rank statistic. The peak value of the scatter plot indicates that when the grouping threshold is set to 0.52, the standard log-rank statistic is the largest. Furthermore, these two groups had the most significant difference in the OS rate. (C) Scatter plot of the *P* value of the survival analysis against the grouping threshold. The dotted line represents the best threshold. When the group threshold was set to 0.52, the *P* value obtained by the log-rank survival analysis was the smallest, and furthermore, the rank statistic reached its peak.

Abbreviation: OS, overall survival.

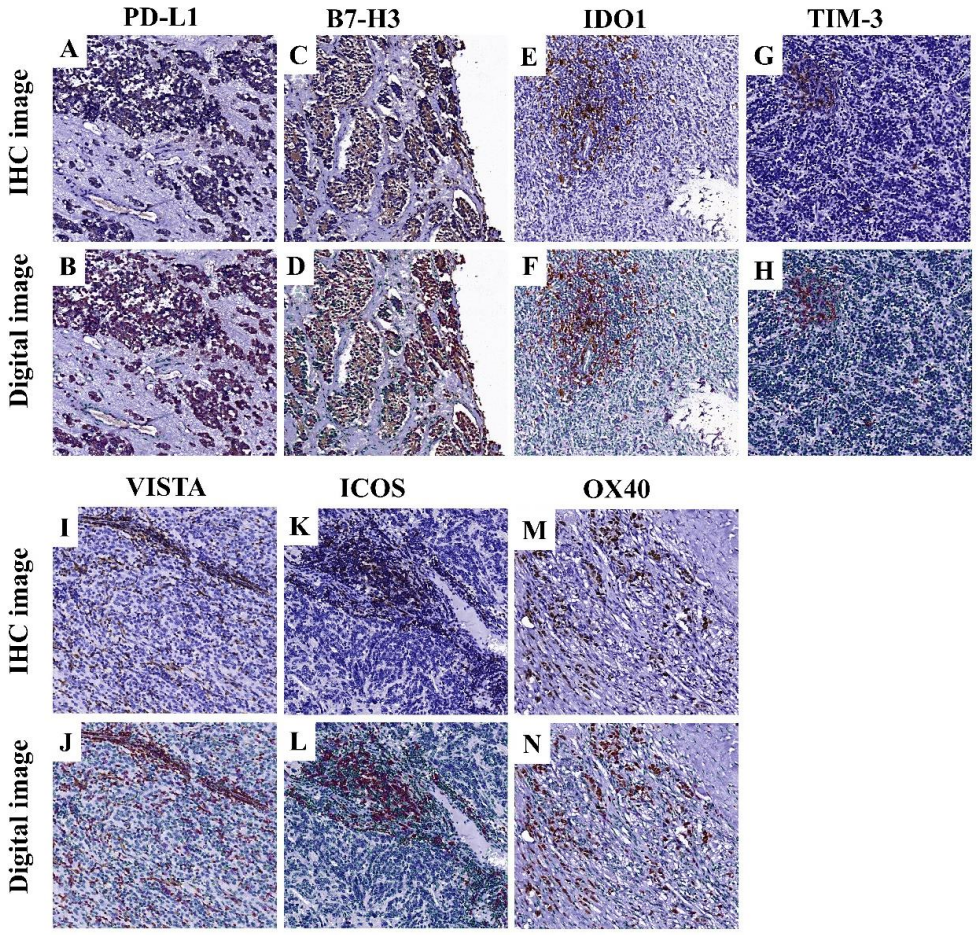

Supplementary Figure S4. Representative immunohistochemistry images of PD-L1, B7-H3, IDO1, TIM-3, VISTA, ICOS and OX40 expression (A, C, E, G, I, K, and M) and corresponding visual nucleus segmentation images in red colour as positive and green colour as negative using digital pathology (B, D, F, H, J, L, and N).

Abbreviations: PD-L1, programmed death ligand 1; IDO1, indoleamine-pyrrole 2,3-dioxygenase 1; TIM-3, T cell immunoglobulin and mucin domain containing-3; ICOS, inducible costimulatory molecule; OX40, costimulatory molecule 40.

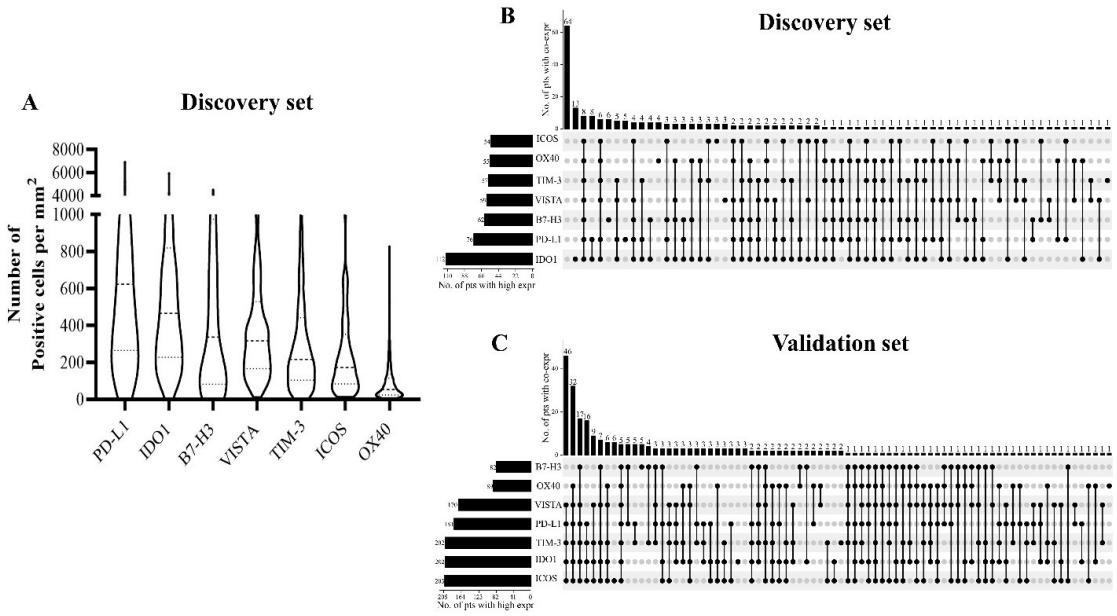

Supplementary Figure S5: The expression of positive cells of seven immune checkpoints and coexpression patterns in the discovery and validation sets. (A) The median number with IQR showing the expression level of seven immune checkpoints calculated by digital pathology in the discovery set (n = 212). UpSet plots showing the coexpression pattern of seven immune checkpoints in the discovery set (B) and validation set (C). The horizontal bars on the left show the number of patients with a high expression of each immune checkpoint. The black beads on the bottom right indicate a high expression of corresponding checkpoints, and the grey beads indicate a low expression of corresponding checkpoints. The black beads connected by the black lines represent the coexpression of the corresponding checkpoints with a high expression status. The vertical bars on the top right show the number of patients with coexpression.

Abbreviations: NB, neuroblastoma; IQR, interquartile range; PD-L1, programmed death ligand 1; IDO1, indoleamine-pyrrole 2,3-dioxygenase 1; TIM-3, T cell immunoglobulin and mucin domain containing-3; ICOS, inducible costimulatory molecule; OX40: costimulatory molecule 40.

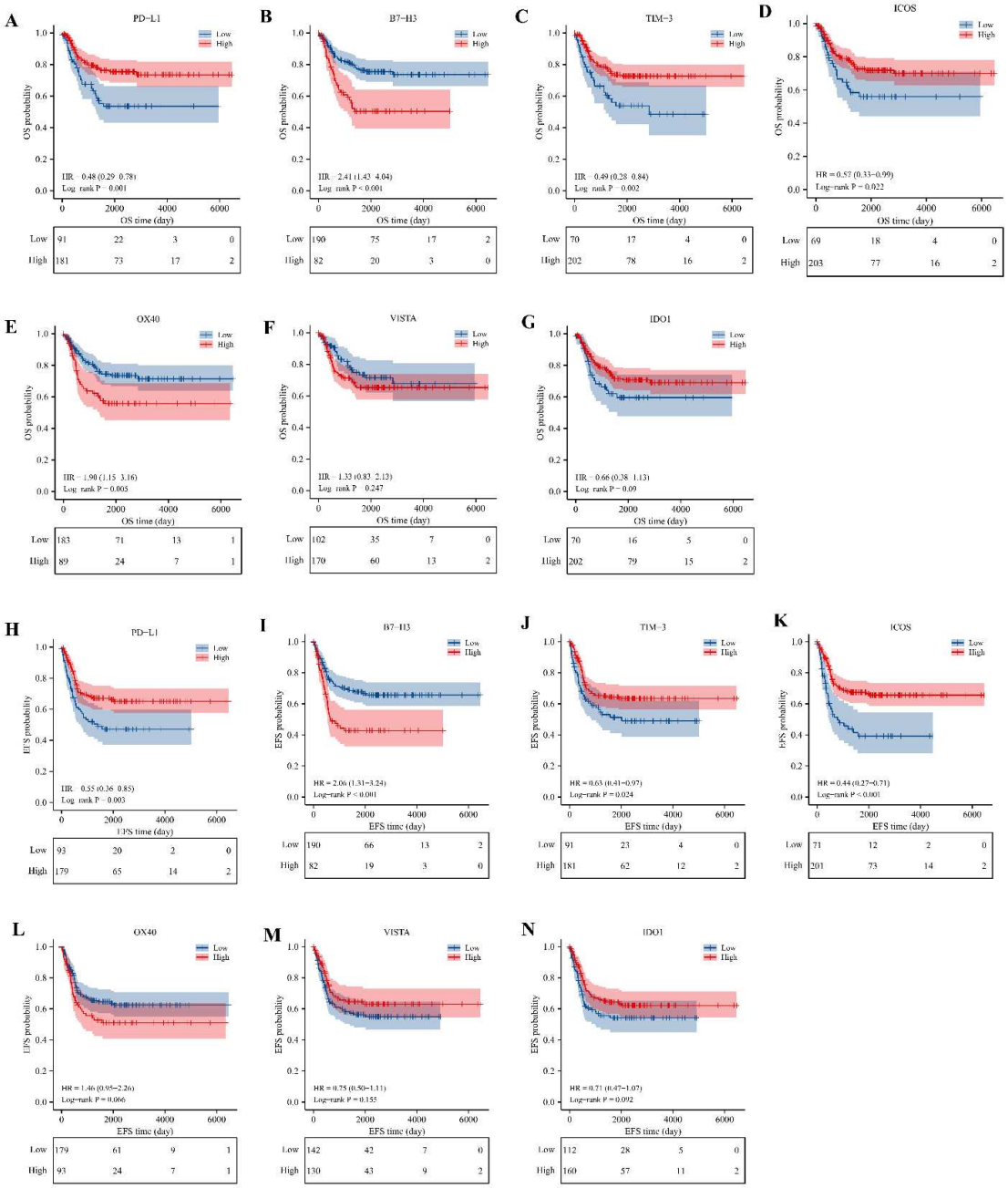

Supplementary Figure S6. Survival analysis of B7-H3, PD-L1, OX40, TIM-3, ICOS, VISTA and IDO1 expression in NB patients in the validation set (n = 272). Kaplan–Meier survival curves were generated according to the high and low expression of B7-H3, PD-L1, OX40, TIM-3, ICOS, VISTA and IDO1 (OS: A, B, C, D, E, F and G; EFS: H, I, J, K, L, M and N). *P* values were calculated by the log-rank test.

Abbreviations: NB, neuroblastoma; OS, overall survival; EFS, event-free survival; PD-L1, programmed death ligand 1; IDO1, indoleamine-pyrrole 2,3-dioxygenase 1; TIM-3, T cell immunoglobulin and mucin domain containing-3; OX40, costimulatory molecule 40; ICOS, inducible costimulatory molecule.

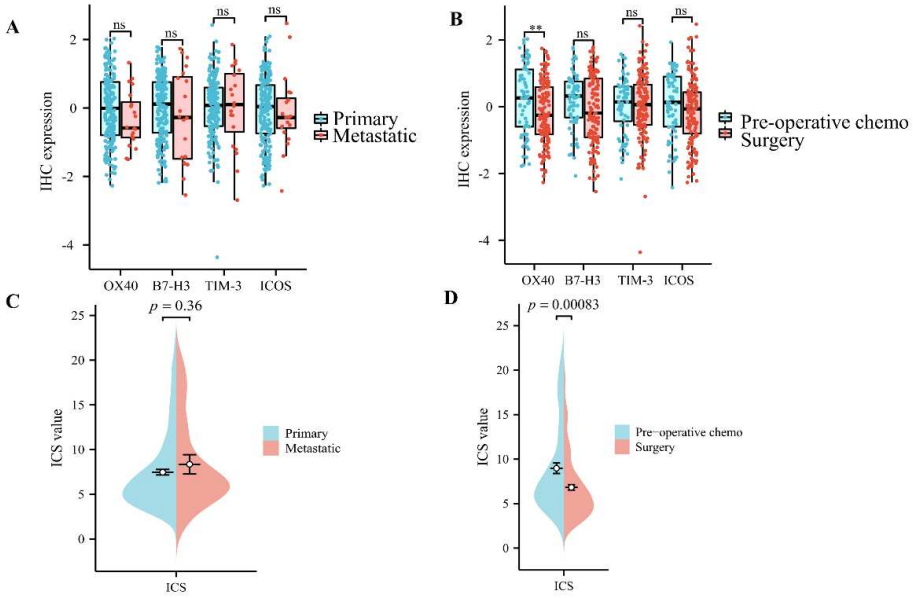

Supplementary Figure S7. The expression difference of the four immune checkpoints in primary and metastatic tumors (A), as well as in tumors first treated with surgery and pre-operative chemo strategies (B). Subsequently, the difference of the ICS value in primary tumors compared with the metastatic tumors (C), and tumors first treated with surgery and pre-operative chemo strategies (D), respectively. **P < 0.01; ns, not significant.

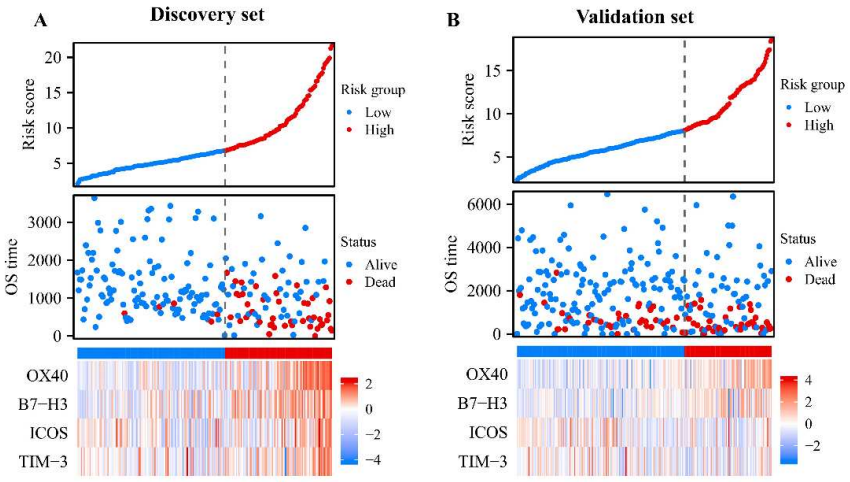

Supplementary Figure S8. The relationship between different risk scores and patients' follow-up time, events, and gene expression levels and an increase in the risk scores (from left to right on the X axis, see the top figure), the survival rate of patients obviously decreased (see the middle figure) and was accompanied by a higher expression of these immune checkpoints (see the bottom figure) in the discovery set (A) and validation set (B).

Abbreviations: OS, overall survival; TIM-3, T cell immunoglobulin and mucin domain containing-3; ICOS, inducible costimulatory molecule; OX40, costimulatory molecule 40.

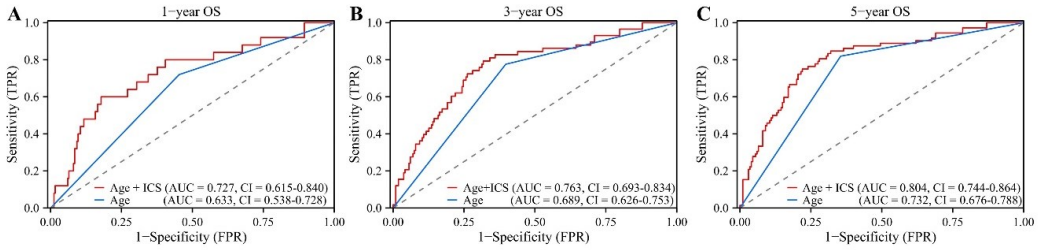

Supplementary Figure S9. Comparisons of the sensitivity and specificity for predicting 1-year, 3-year and 5-year OS in the validation set. ROC curves of nomograms A (ICS + age) and B (age only) as predictors of 1-year (A), 3-year (B) and 5-year (C) OS.

Abbreviations: OS, overall survival; ICS, immune checkpoint-based signature; ROC, receiver operating characteristic.

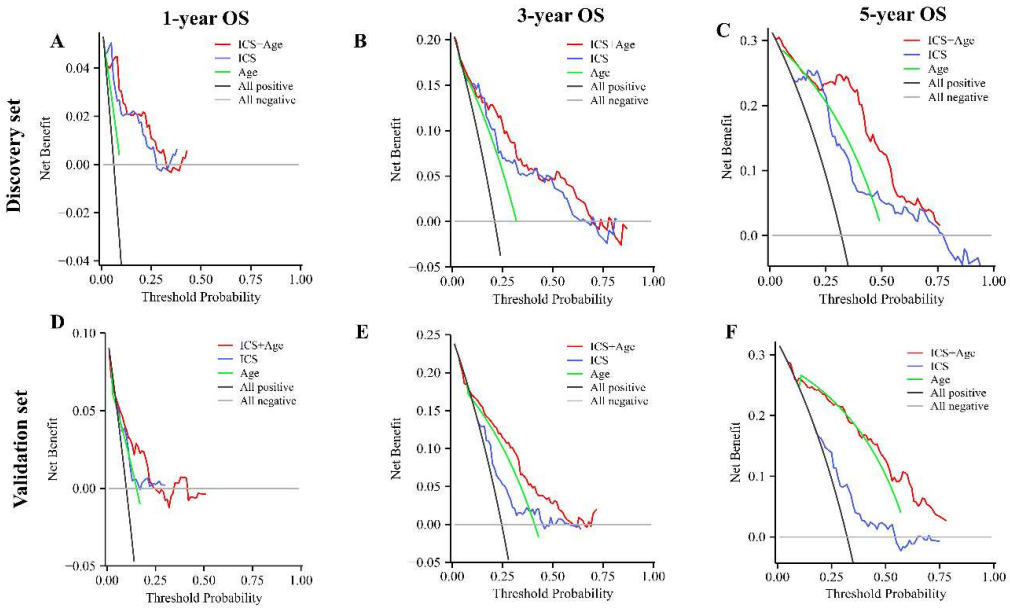

Supplementary Figure S10. DCA curves showing the performance (net benefit) of each model in predicting 1-year, 3-year and 5-year OS in the discovery (top panel) and validation sets (bottom panel). The y-axis represents the net benefit, which is the probability of true positives minus the probability of false positives weighted for the threshold probability. The black line shows the net benefit of considering all patients positive; the solid grey horizontal line considers all patients negative. In the discovery set, the net benefit in the ICS + age model would show advantages over the ICS and age only in predicting 1-year (A), 3-year (B) and 5-year (C) OS, which were confirmed in the validation set (D, E and F, respectively). The net benefit is calculated as (proportion of true positives) – (proportion of false-positives) * the threshold probability/(1− the threshold probability).

Abbreviations: DCA, decision curve analysis; ICS, immune checkpoint-based signature; OS, overall survival.